Environment International 126 (2019) 268–278

Contents lists available at ScienceDirect

Environment International

journal homepage: www.elsevier.com/locate/envint

Evaluation of the taxonomic and functional variation of freshwater plankton communities induced by trace amounts of the antibiotic ciprofloxacin

Tao Lu[a], Youchao Zhu[a], Mingjing Ke[a], W.J.G.M. Peijnenburg[b,c], Meng Zhang[a], Tingzhang Wang[d], Jun Chen[e], Haifeng Qian[a,*]

[a] College of Environment, Zhejiang University of Technology, Hangzhou 310032, China
[b] Institute of Environmental Sciences (CML), Leiden University, RA, Leiden 2300, the Netherlands
[c] National Institute of Public Health and the Environment (RIVM), Center for Safety of Substances and Products, P.O. Box 1, Bilthoven, the Netherlands
[d] Key laboratory of microbial technology and bioinformatics of Zhejiang Province, Hangzhou 310012, China.
[e] College of Biological and Environmental Engineering, Zhejiang Shuren University, Hangzhou 310021, China

ARTICLE INFO

Handling Editor: Yong-Guan Zhu

Keywords:
Ciprofloxacin
Cyanobacteria
Meta-transcriptomic analysis
High-throughput sequencing
Freshwater microbiome

ABSTRACT

Ciprofloxacin (CIP), one of the most frequently detected antibiotics in water systems, has become an aquatic contaminant because of improper disposal and excretion by humans and animals. It is still unknown how trace amounts of CIP affect the aquatic microbial community diversity and function. We therefore investigated the effects of CIP on the structure and function of freshwater microbial communities via 16S/18S rRNA gene sequencing and metatranscriptomic analyses. CIP treatment (7 μg/L) did not significantly alter the physical and chemical condition of the water body as well as the composition of the main species in the community, but slightly increased the relative abundance of cyanobacteria and decreased the relative abundance of eukaryotes. Metatranscriptomic results showed that bacteria enhanced their phosphorus transport and photosynthesis after CIP exposure. The replication, transcription, translation and cell proliferation were all suppressed in eukaryotes, while the bacteria were not affected in any of these aspects. This interesting phenomenon was the exact opposite to both the antibacterial property of CIP and its safety for eukaryotes. We hypothesize that reciprocal and antagonistic interactions in the microcosm both contribute to this result: cyanobacteria may enhance their tolerance to CIP through benefiting from cross-feeding and some secreted substances that withstand bacterial CIP stress would also affect eukaryotic growth. The present study thus indicates that a detailed assessment of the aquatic ecotoxicity of CIP is essential, as the effects of CIP are much more complicated in microbial communities than in monocultures. CIP will continue to be an environmental contaminant due to its wide usage and production and more attention should be given to the negative effects of antibiotics as well as other bioactive pollutants on aquatic environments.

1. Introduction

Antibiotics are widely used in agriculture and animal husbandry, as well as in medical treatment fields to combat diseases affecting plants, animals and humans (Keeney et al., 2014; Su et al., 2018). Wastewater treatment plants often fail to completely eliminate antibiotics, causing them to eventually flow into surface waters (Tahrani et al., 2016; An et al., 2018a, 2018b). In agriculture, the manure usually contains antibiotics, which may also be introduced into the environment through surface runoff (Kulesza et al., 2016; Zhu et al., 2013, 2017). Aquaculture activities are another source of antibiotics for the aquatic environment (Zheng et al., 2012). China is the largest consumer of antibiotics in the world. In 2013, there were 92,700 tons of antibiotics consumed in China, of which 53,800 tons eventually entered the receiving environment (Zhang et al., 2015).

Ciprofloxacin (CIP) is one of the most frequently detected antibiotics in China, which was commonly used both for veterinary and human purposes. In natural lakes, the concentrations of CIP are usually below 100 ng/L, but higher concentrations were also reported (Jiang et al., 2014; Zhang et al., 2017; Hanna et al., 2018). A maximum concentration of 7.49 and 5.93 μg/L was detected in wastewater from an animal farm and in surface water in Suzhou, near Lake Taihu, the third large lake of China (Wei et al., 2012). Many freshwater lakes, like Lake Taihu, have already suffered from eutrophication for years, while the presence of residuals of antibiotics like CIP would even increase the level of contamination.

* Corresponding author.
E-mail address: hfqian@zjut.edu.cn (H. Qian).

https://doi.org/10.1016/j.envint.2019.02.050
Received 25 December 2018; Received in revised form 20 February 2019; Accepted 20 February 2019

CIP has broad-spectrum antibacterial activity against Gram-negative and positive bacteria by inhibiting the activity of bacterial DNA gyrase and interfering bacterial DNA replication (Wallace et al., 2018). It is demonstrated that the inhibition of bacteria by CIP is in general stronger than that of eukaryotes. For instance, Ebert et al. (2011) found that CIP is more toxic to the cyanobacteria *Anabaena flos-aquae* as compared to the monocotyledonous macrophyte *Lemna minor* and the green alga *Desmodesmus subspicatus*, the EC_{50}-values (i.e. the 50% effect concentration) of them were 10.2, 62.5, and 8042 μg/L respectively, and for the dicotyledonous macrophyte *Myriophyllum spicatum* the 50% inhibition was not observed in the high concentration of 63,530 μg/L. European researchers conducted an environmental risk assessment on CIP, and found that the chronic EC_{50} of CIP for the freshwater cyanobacteria *Microcystis aeruginosa* is 5 μg/L whereas the lowest no observed effect concentration for the eukaryote *Daphnia magna* is higher than 60 mg/L (Hallingsørensen et al., 2000).

However, once CIP enters the water environment, not only a single alga is observed, but the entire plankton community, including algae, bacteria, fungi, zooplankton and other species. Due to the complexity of a community ecosystem, the exposure-response model of a community will be much more complex than a single species model. Only limited research explored the community effects of CIP till now. Johansson et al. (2014) found that CIP blocked carbon source utilization of natural marine biofilms at a concentration of 8.6 μg/L. Wilson et al. (2003) found that environmentally relevant concentrations (0.015–1.5 μg/L) of CIP caused significant changes in the suspended and attached algal community structure at the upstream and downstream sites of a wastewater treatment plant and led to a continuous decline in algal richness. However, these studies are relatively preliminary, and research on the mechanisms underlying the functional response of microbial communities at the molecular level has barely started.

Microbial communities in water are regulated by various environmental factors, including pH, temperature, nutrients, and contaminants. These microorganisms are carriers of ecosystem energy flow, and the community composition may cause functional variation. The emergence of 16S/18S rRNA gene amplicon sequencing allows researchers to gain insight into the dynamics of microbial communities more quickly and accurately than traditional community identification methods. Meta-transcriptomics have been proven to be a powerful tool for identifying different cellular levels of microbial communities in the context of all metabolic activities. Here, the combination of 16S/18S rRNA gene amplicon sequencing and metatranscriptome analysis was used to study the structural and functional response of aquatic microbial communities to an environmentally relevant concentration of CIP in microcosms of a eutrophic freshwater Chinese lake.

2. Material and methods

2.1. Plankton source and culture

Lake Taihu is the third largest freshwater lake in China. Cyanobacteria blooms occur every summer, and the blooms are mainly comprised of *Microcystis* spp. The Meiliang Bay is the most severe bloom sites of Lake Taihu. The annual total nitrogen concentrations range from 1.24 mg/L in the central lake to 9.48 mg/L in Meiliang Bay, and the total phosphorus (TP) concentrations in Meiliang Bay range from 0.08 to 0.32 mg/L (Xu et al., 2010). Plankton samples were collected at Meiliang Bay of lake Taihu, Wuxi, China (30°55′40″–31°32′58″N, 119°52′32″–120°36′10″ E) in November 2017, when the bloom was diminished. Surface water at a depth of 0.5 m were collected by a glass collection unit and delivered to the laboratory as soon as possible, and were then inoculated into medium within 24 h. The collected plankton samples were filtered using a filter with a pore size of 0.45 μm, and the plankton on the membrane was inoculated into a modified BG11 medium. The modified BG-11 medium contains 1/10 of the total N and P content of the original BG-11 medium, namely 24.7 mg N/L and 0.54 mg P/L (the composition of the medium is shown in Table S1). The plankton was cultured under a 12:12 hour light:dark cycle of cool-white fluorescent light (46 μmol m^{-2} s^{-1}) in 2 L-beakers. The temperature was controlled at 25 ± 0.5 °C, and the beaker mouths were covered with absorbent gauzes to allow microbial respiration and prevent contamination by external microbes.

2.2. Experimental design

Tested single algal species including green alga *Chlorella pyrenoidosa* (FACHB-9), a *Monoraphidium* sp. (FACHB-1853), and the cyanobacteria *Microcystis aeruginosa* (FACHB-905), *Synechococcus 7942* (FACHB-805), and a *Pseudanabaena* sp. (FACHB-2209) were obtained from the Institute of Hydrobiology at the Chinese Academy of Sciences (Hubei, China). In our 7-day preliminary experiment, 1–9 μg/L of CIP inhibited the growth of *M. aeruginosa* to varying degrees. We tested 7 μg/L of CIP on other cyanobacteria and green algae species, and found that the maximum inhibition rate of the growth of a cyanobacteria (*Synechococcus* 7942) was only 14.7%, and no effect was found on the growth of two green algae *Chlorella pyrenoidosa* and a *Monoraphidium* sp. at a concentration of 7 μg/L of CIP. We therefore supposed that this concentration would alter the composition of microbial communities to some extent. We constructed microcosms in 2 L-beakers containing 1.8 L of medium, and adjusted the initial optical density of the plankton communities at the wavelength of 680 nm (OD_{680}) to 0.01 in order to unify the initial algal biomass (approximately 0.07 mg Chl *a*/L), which was close to the biomass of the original water samples. In addition, the initial pH was adjusted to 7.0 to obtain a neutral environment. Plankton communities exposed to 7 μg/L of CIP were set as the treatment group, and a control group was established consisting of the same communities without CIP addition, each in triplicate. All materials were sterilized at 121 °C for 30 min before use in the experiments. Water quality parameters including pH, electrical conductivity (EC), TP, dissolved nitrate-nitrogen (NO_3^--N) and algal growth parameters which include Chl *a* and phycocyanin (PC) were measured directly or collected for determination at approximately 9 am at 0, 1, 3, 5, 7, 10, 13, and 15 days. Each 100 mL volume of water sample was used for 16S/18S rRNA gene amplicon sequencing after 5, 10 and 15 days of exposure, and 1000 mL of water sample was used for the meta-transcriptomic sequencing after 15 days. Approximately 1.6, 1.4 and 0.1 L of water sample was left in the beaker after 5, 10 and 15 days due to sampling and evaporation.

2.3. Determination of pH, phycocyanin, EC, NO_3^--N, TP, Chl a, and PC

pH and EC were determined directly by using a pH meter (FE-20, Mettler Toledo®, Colombus, USA) and an electrical conductivity meter (InPro 7100i/12/120, Mettler Toledo®, Colombus, USA). NO_3^--N and TP concentrations in the medium were measured after 5 mL of plankton was filtered using a 0.45 μm pore size filter according to the methods described by Song et al. (2017). The growth of phytoplankton is reflected by the concentration of Chl *a* and PC. Chl *a* is widely used as an indicator of the biomass of phytoplankton (Kasprzak et al., 2008; Du et al., 2019), and PC is used as an indicator of the biomass of cyanobacteria (Woźniak et al., 2016). Both Chl *a* and PC were determined with 30 mL of water sample. Chl *a* was extracted and determined as described by Lu et al. (2018a). PC was extracted by a sodium phosphate buffer and determined as described by Silveira et al. (2007).

2.4. 16S/18S rRNA gene amplicon sequencing

16S/18S rRNA gene amplicon sequencing was performed on the 5-, 10-, and 15-day samples. Microbial DNA was extracted by using a cador Pathogen 96 QIAcube HT Kit. The DNA concentration was detected using a Qubit 2.0 Fluorometer (Invitrogen, Carlsbad, CA). The 16S/18S rRNA gene sequencing library was constructed using the MetaVx™

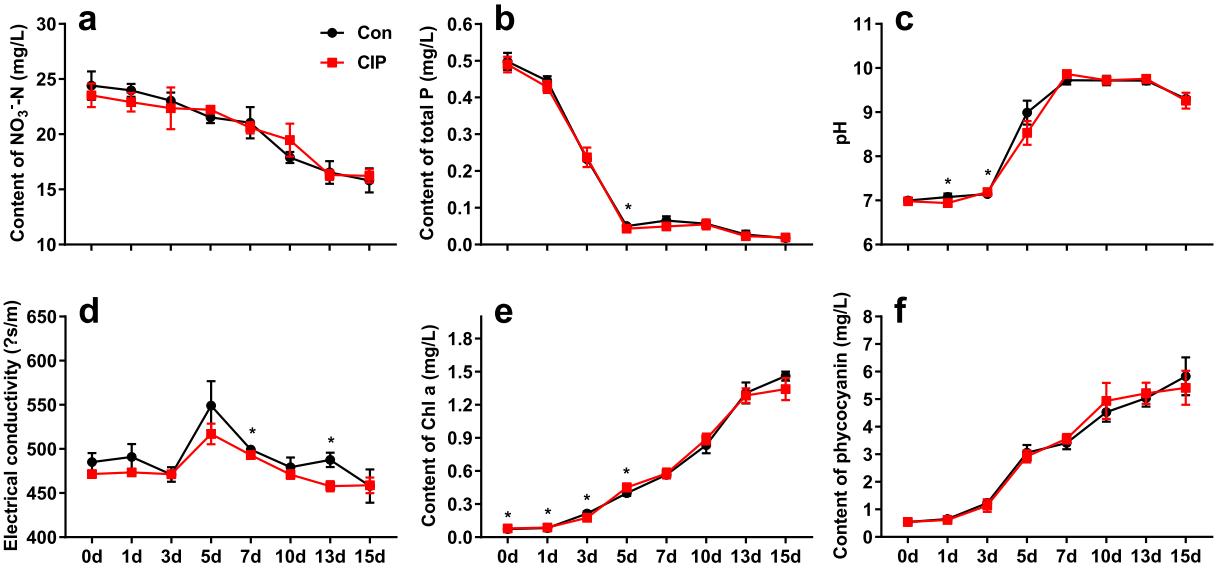

Fig. 1. Phytoplankton growth and water quality parameters of the control and ciprofloxacin (CIP) treated microcosms during the 15-day culture. (a) Nitrate-nitrogen (NO_3^--N) and (b) total phosphorus (TP) concentrations, (c) pH and (d) electrical conductivity (EC), (e) chlorophyll *a* (Chl *a*) and (f) phycocyanin (PC) of the microcosms. Asterisks represent statistically significant ($P < 0.05$).

Library Construction Kit (GENEWIZ, Inc., South Plainfield, NJ, USA). For 16S rRNA gene sequencing, two highly variable regions, V3 and V4, were amplified using an upstream primer comprising the "CCTACGGRRBGCASCAGKVRVGAAT" sequence and a downstream primer comprising the "GGACTACNVGGGTWTCTAATCC" sequence. For 18S rRNA gene sequencing, two highly variable regions, V7 and V8, were amplified using an upstream primer comprising the "CGWTAACGAACGAG" sequence and a downstream primer comprising the "AICCATTCAATCGG" sequence. After the DNA library was constructed, PE300 paired-end sequencing was conducted on Illumina MiSeq (Illumina, San Diego, CA, USA) according to the instructions. Clean reads were obtained after removal of adapters and low quality sequences from raw reads. Sequence clustering was conducted by using VSEARCH (1.9.6). Sequences with similarity above 97% were identified as one OTU. Silva 128 was selected as the reference database in annotation. The alpha diversity indices including Shannon, Chao1, etc. were calculated based on OTUs. Principal component analysis (PCA) was used to compare bacterial community differences between the control and treatment groups. The 16S rRNA gene amplicon sequencing and basic analysis were performed by GENEWIZ (Suzhou, China). The raw data have been submitted to the NCBI Sequence Read Archive (SRA) database with accession numbers SAMN10956580 to SAMN10956597 (16S), and SAMN10956598 to SAMN10956615(18S).

2.5. Metatranscriptome sequencing

To analyze the effects of CIP at the transcriptional level of planktonic communities, metatranscriptome sequencing was performed on samples on the 15th day. Microbial RNA was extracted by the GeneTool Total RNA Isolation Kit. Then an Agilent 2100 Bioanalyzer (Agilent Technologies, Palo Alto, CA, USA), NanoDrop (Thermo Fisher Scientific Inc.) and 1% agarose electrophoresis were used to determine the RNA concentration and quality. One microgram total RNA with RIN ≥ 7 was used for library construction using the NEBNext® UltraTM Directional RNA Library Prep Kit for Illumina®. We refer to the Supplemental materials for an overview of specific procedures for library construction. After the library was constructed, 2 × 150 bp pair-end sequencing (PE) was performed according to the Illumina HiSeq (Illumina, San Diego, CA, USA) instrument instruction manual. Sequence information was obtained by HiSeq Control Software (HCS) + OLB + GAPipeline-1.6 (Illumina). Clean reads were obtained by removing low-quality reads, N rich reads and adapter-polluted reads from the raw reads using cutadapt (v1.9.1). Assembly software Trinity (v2.2.0) was used to assemble clean reads to unigenes. BLAST (version 2.2.31 +) was used to annotate unigenes with the KEGG database. FPKM (Fragment Per Kilo bases per Million reads) was calculated by RSEM (V 1.2.4) to analyze gene expression of unigenes. Differential gene expression folds ≥ 2 and FDR ≤ 0.05 were set as thresholds to determine if genes were differentially expressed. Hierarchical clustering analysis and KEGG pathway enrichment analysis were conducted based on FPKM. The sequencing and basic analysis of the metatranscriptome was performed by GENEWIZ (Suzhou, China). The raw data have been submitted to the NCBI Sequence Read Archive (SRA) database with accession numbers SAMN10638944 to SAMN10638949.

2.6. Determination of CIP concentration

Water sample was filtered by a 0.45 μm pore size filter membrane, then CIP was extracted from the filtrate by a C18 solid phase extraction column and determined by high performance liquid chromatography (HPLC) (Shimadzu CBM-20A, Japan) equipped with a fluorescence detector (Shimadzu RF-20A, Japan). The mobile phase is 0.05 M phosphoric acid (pH was adjusted to 2.4 by triethylamine): HPLC-grade acetonitrile (v:v) = 82:18. The excitation wavelength of the fluorescence detector is 280 nm and the emission wavelength is 450 nm. The HPLC column is WondaSil C18-WR (4.6 × 250 mm, 5 μm) with a flow rate of 0.8 mL/min. The injection volume is 20 μL. The column temperature is room temperature.

2.7. Statistical analyses

The statistical significance of physiological and physical data was analyzed using a one-way analysis of variance (ANOVA) (StatView 5.0 program), and the statistical significance of metatranscriptome data was analyzed using the Student's *t*-test (Two-tailed, hypothesis under heteroscedasticity). A probability (P) value of < 0.05 was considered significant. The data in the figures are presented as mean ± standard deviation (SD).

3. Results and discussion

3.1. Nutrients, Chl a, PC and CIP concentrations

In the control group, with the number of culturing days increasing, the NO_3^--N content in the medium decreased from the initial 24.40 mg/L to 15.81 mg/L on the 15th day (Fig. 1), while the TP content decreased rapidly from the initial 0.48 mg/L to 0.050 mg/L after the first 5 days, after which the TP content slowly decreased to 0.018 mg/L on the final culture day. When there is sufficient N, the phytoplankton will continuously grow until the P concentration drops to approximately 0.20 mg/L (Xu et al., 2010). The pH value rose rapidly from the initial 7.0 to above 9.0, and stabilized between 9.0 and 10.0 after 5 days of culture. This phenomenon was in accordance with the pH of Lake Taihu which ranged from 7.73 in February to 9.53 in July during 3 years (Xu et al., 2010). The pH increase is caused by fixation of CO_2 by cyanobacteria, which reduces dissolved carbon dioxide and increases the proportion of bicarbonate and carbonate. This process will create a concentration gradient across the air-water interface and causes a greater influx of CO_2, and thus in turn facilitates cyanobacteria to grow (Qian et al., 2017; Visser et al., 2016). EC was relatively stable throughout the culture process. It is to be noted that these water quality parameters did not differ significantly at the same time point between the control and treatment (Fig. 1), suggesting that the CIP did not appear to have any negative effects on the physical condition of the water environment and did not influence the N and P utilization rate of the microbial communities.

The residual test was carried out with an initial CIP concentration of 70 μg/L in the microcosm. Results show that the CIP concentrations at 5 d and 10 d were still as high as 56.0 and 47.6 μg/L, respectively, indicating that CIP was relatively stable in the water environment, which is in line with the literature (Ben et al., 2018; Jia et al., 2018).

3.2. Changes in the composition and diversity of bacterial community

16S/18S rRNA gene sequencing was performed to identify the composition of the microbial community of the microcosms (Dataset 1). The results of 16S rRNA gene sequencing taxonomy at the class level showed that the community structure changed drastically over time (Fig. 2a). On the 5th day, *Betaproteobacteria* (55.2%) were the dominant class in the control group, and they were increased to 66.9% in the treatment group. These *Betaproteobacteria* are mainly consisting of the genus *Methylophaga* (96.6 and 98.2% of the control and the treatment group), but they decreased rapidly with the cultivation process. On the 10th day, *Sphingobacteriia* (40.0%) were the predominant class in the control group, but they decreased after CIP treatment, while *Alphaproteobacteria* increased from 29.7% to 42.8%, becoming the predominant class in the treatment group. On the 15th day, *Cyanobacteria* (61.2%) were the predominant class, representing the occurrence of a cyanobacteria bloom, and they slightly increased to 64.5% after treatment. Referring to the RNA annotation of the metatranscriptome (Fig. 3c), the cyanobacteria were dominated by the genus *Pseudanabaena* (71.3% of the *Cyanobacteria* in the control group), *Synechocystis* (3.0%), and *Synechococcus* (3.3%), all of which are microcystins (MCs)-producers (Oudra et al., 2002; Barboza et al., 2017). Interestingly, although some bacteria such as *Thauera* from *Betaproteobacteria* were severely inhibited, the addition of CIP did not inhibit the composition of cyanobacteria (Fig. 3c, d). *Pseudanabaena* and *Synechococcus* are not sensitive to CIP. The maximum inhibition rate of 7 μg/L of CIP against *Synechococcus 7942* and *Pseudanabaena* sp. was only 14.7% and 12.3%, respectively (Fig. S1), which could be an important reason that the cyanobacteria structure did not change significantly.

Environmental factors are critical to the survival of microorganisms, and are able to alter the microbial community structure (Liao et al., 2018; Lu et al., 2018b). The increase in pH (Fig. 1c) was likely to affect the chemical speciation of CIP, as CIP displays pH-dependent chemical speciation (pKa's of 6.3 and 8.8) affecting the charge of the molecule and therefore its ability to pass biological membranes. CIP bioavailability and toxicity may therefore depend strongly on pH which increased dramatically from 7 to almost 10 during the microcosm incubations. This could be an important reason for the large difference of the composition of the microbial community between 5 and 10 days as compared to the controls. Besides, other factors such as lack of available substrate and light obscuration caused by a surge in biomass formed by cyanobacteria might cause the death of some microorganisms. For example, the genus *Methylophaga* consists of strict aerobic, moderately halophilic bacteria which cannot synthesize vitamin B_{12} by themselves. In addition to fructose, one-carbon compounds are their only growth substrate (Doronina et al., 2003). Failure to meet any of the conditions that are essential for growth could lead to their death in this study. A recent study found that the genus *Methylophaga* consists of potentially high-efficient MCs-degrading bacteria (Mou et al., 2013). Their demise might be beneficial to the accumulation of MCs, causing potential pressure on the remaining aquatic microbes.

Although it seems that the main species of the bacterial community did not change significantly, we hypothesized that the diversity of the community might still undergo potential changes due to some rare species. Community diversity analysis was calculated based on the OTU level. The Shannon and Simpson indices reflect the diversity and uniformity of the community, while the ACE and Chao1 indices reflect the richness, which indicates the estimated number of actual species (Qian et al., 2018). Compared with the control group, the 15-day ACE and Chao1 indices in the treatment group decreased significantly, and the Shannon and Simpson diversity indices also slightly decreased (Fig. 4a), indicating the decline in the richness and diversity of bacterial communities. Principal component analysis (PCA) showed that (Fig. 4b),

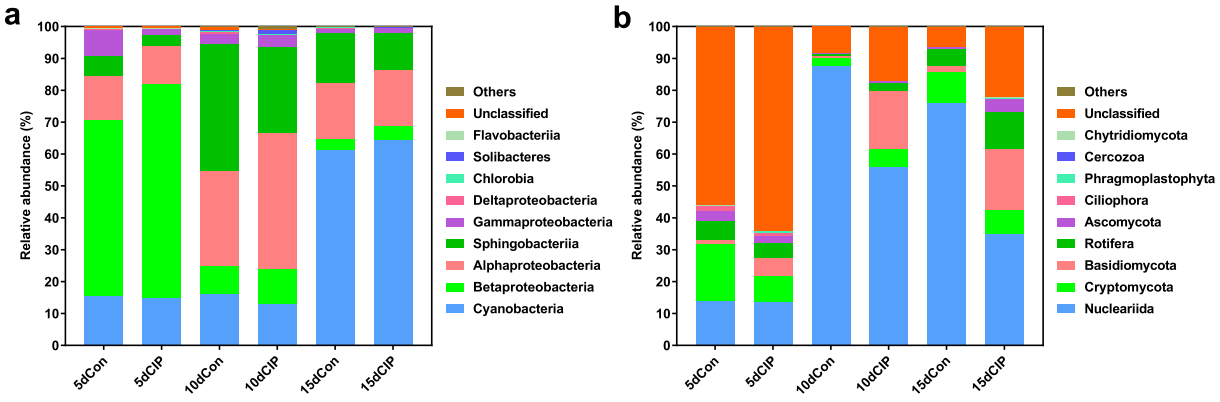

Fig. 2. Mean relative abundance of species taxonomy of the control and CIP treated samples for 5, 10, and 15 days derived from (a) 16S rRNA gene sequencing analysis at class level and (b) 18S rRNA gene sequencing analysis at the phylum level.

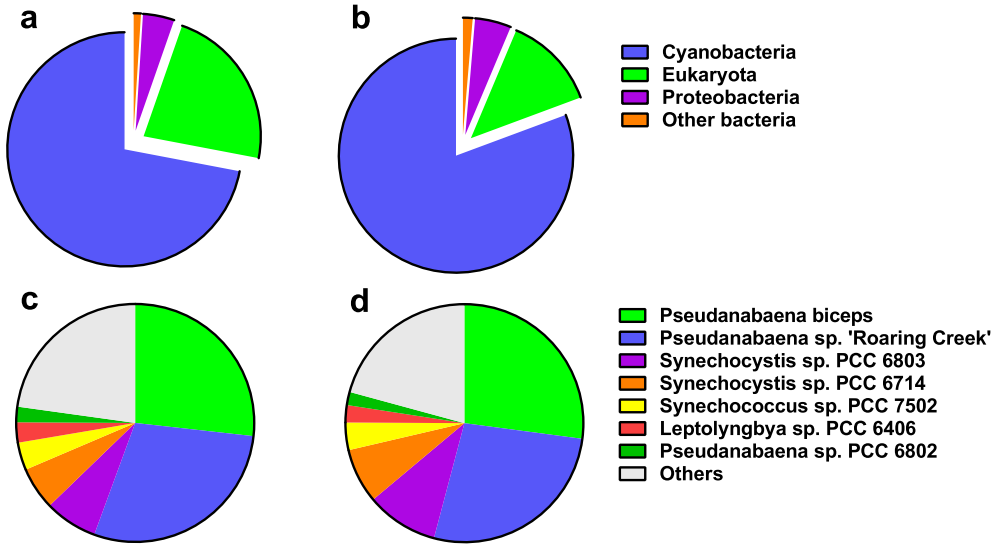

Fig. 3. Metatranscriptome analysis derived mean relative abundance of RNA sequencing annotation of (a) the control and (b) the CIP treated group at the phylum level, and (c) the control and (d) the CIP treated group at the species level belonging to the phylum *Cyanobacteria*.

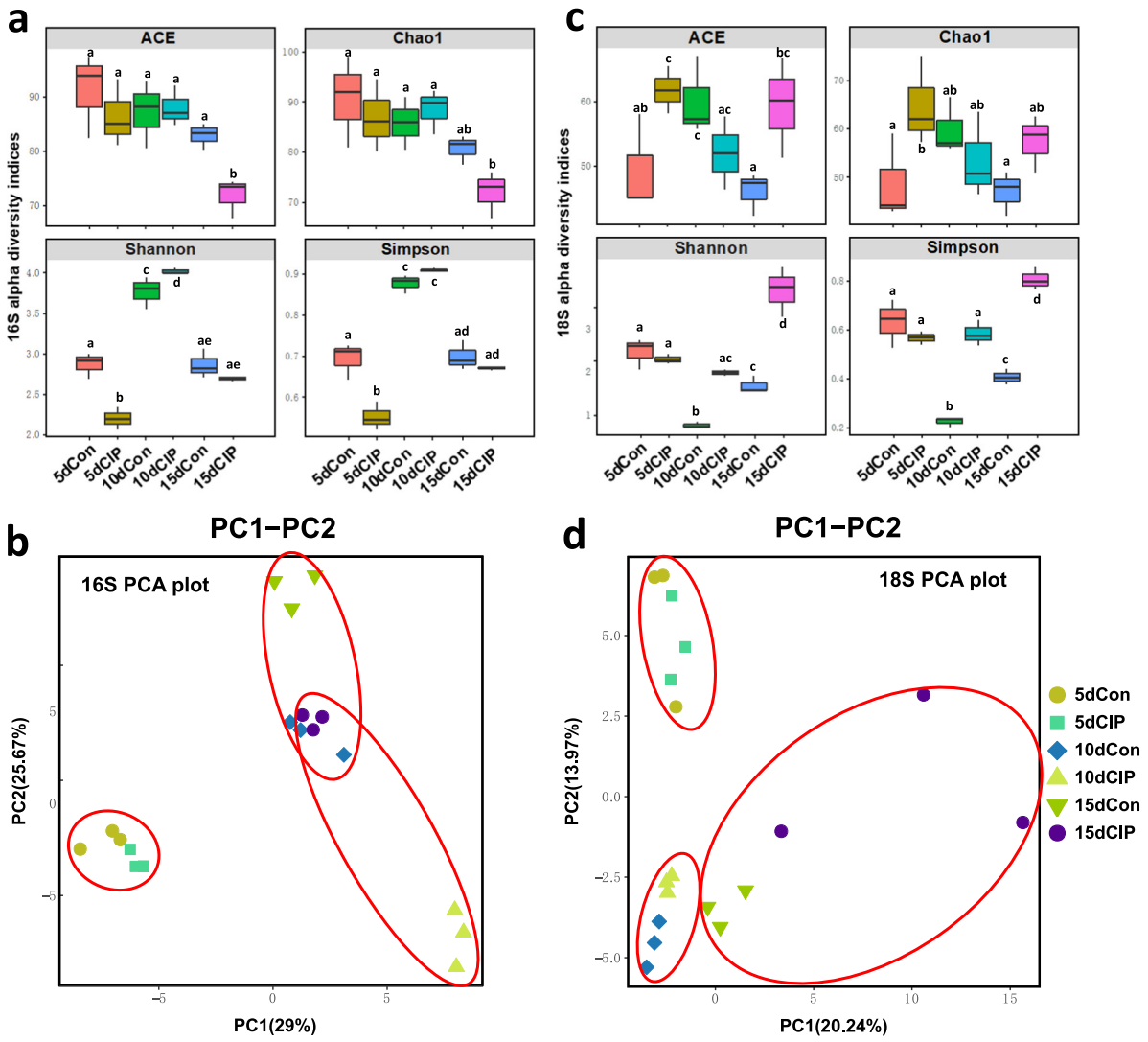

Fig. 4. (a) Alpha indices including ACE, Chao1, Shannon, and Simpson and (b) principal component analysis (PCA) based on OTUs of the control and CIP treated samples derived from 16S rRNA gene sequencing analysis for 5, 10, and 15 days, (c) alpha indices and (d) PCA based on OTUs derived from 18S rRNA gene sequencing analysis. Samples from different days are marked in the circles. Different letters represent statistically significant differences ($P < 0.05$).

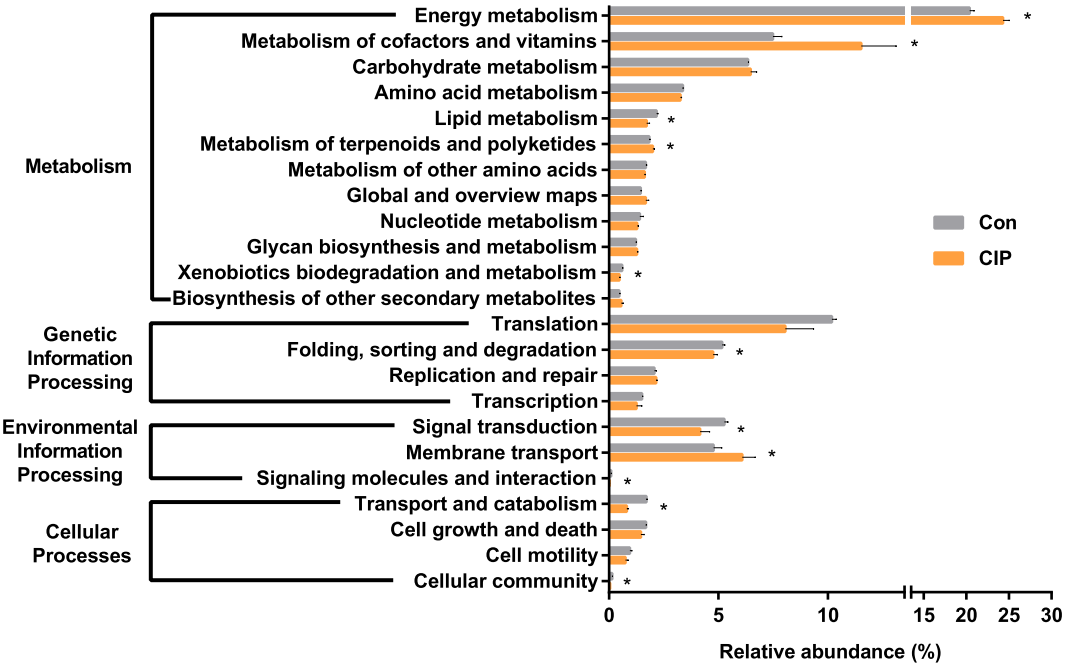

Fig. 5. Relative abundance of metabolic subsystems (KEGG level 2) of the control and CIP treated samples for 15 days based on metatranscriptomic analysis. Asterisks represent statistically significant differences ($P < 0.05$).

(first principal component) PC1 and (second principal component) PC2 together explained a total of 54.67% of the β-diversity. Environmental factors such as nutritional conditions and pH might be populating PC1, affecting the OTU composition at the time-scales used in this study as the 5-day samples were separated from the 10- and 15-day samples. CIP could constitute a major portion of PC2 as it is likely to result in the separation of the control and treatment samples (Fig. 4b). The reduced ACE and Chao1 indices of the treatment group on the 15th day suggested a decrease in the number of species. However, the abundance of the main species in the community did not change significantly, indicating that some relatively rare bacteria might be eliminated by CIP. Since these rare taxa might play an important role in community functioning (Szabó and Itor, 2007), CIP may have adverse effects on the bacterial community diversity and even the functioning.

3.3. Changes in the composition and diversity of the eukaryotic community

Various species were identified in the eukaryotic community, including some protozoa under the phyla *Nucleariida*, *Ciliophora*, metazoans under the phylum *Rotifera*, and fungi under the phyla *Cryptomycota*, *Basidiomycota*, *Ascomycota*, *Chytridiomycota* (Fig. 2b, Dataset 2). There were many phytoplankton grazers, such as some *Nucleariida*, *Rotifera* and *Ciliophora* (Dirren et al., 2017; Liang et al., 2017b; Wang et al., 2017). The parasites under the phylum *Cryptomycota* are usually parasitic in the host of the *Chytridiomycota*. Because the latter can be parasitic in some heterotrophic algae, they play a key role in regulating the population density of phytoplankton, zooplankton and small invertebrates, and in the transfer of matter and energy in the food web (Letcher et al., 2017). The existence of these complex eukaryotic networks suggested complex interrelationships (such as predation, parasitism, competitive relationships, etc.) between eukaryotic communities. In the 10- and 15-day samples, the *Nucleariida* were the most important eukaryote, accounting for 87.7% and 76.1% of the eukaryotic sequence of the control group. The rigid structure of cyanobacteria filaments and toxic secondary metabolites such as MCs scares of many grazers, so toxic filamentous cyanobacteria are more competitive in the presence of grazers. However, the *Nucleariida* can overcome this pray defense mechanism, using toxic filamentous cyanobacteria as a food source (Dirren et al., 2017). Considering the presence of many toxic filamentous cyanobacteria (*Pseudanabaena*) in prokaryotic communities, this could be the main reason for the predominance of *Nucleariida*. In the CIP treated group, the relative abundance of the *Nucleariida* was reduced to 55.8% and 34.8% on the 10th and 15th day, whereas other eukaryotes such as *Rotifera* and *Basidiomycota* increased, leading to the relaxation of the evenness of eukaryotic communities and restoration of the diversity to some extent. This is consistent with the rise in the Shannon and Simpson diversity indices in the 10- and 15-day treatment groups (Fig. 4c). PCA analysis showed that PC1 and PC2 provided a limited contribution to explain the total variance in the data, explaining only a total of 34.21% of the β-diversity. This indicates that the factors that dominated the changes of eukaryotic community were more complicated. The coordinates of the treatment and control group on the 15th day were separated, although not very clearly (Fig. 4d), indicating that CIP still exerted some effects on the eukaryotic community, which could be mostly on *Nucleariida*.

3.4. Overview of metatranscriptome sequencing

In order to compare the global functioning of microbial communities, metatranscriptome sequencing was performed on samples after 15 days of treatment. Sequencing generated a total of 681.3 million (M) of raw reads. According to the quality control report, the Q30 of all samples was > 90%, indicating that the sequencing data is of good quality and the results are reliable. A total of 677.9 million (M) of clean reads were obtained. The FPKM values were lower in the treatment group compared to the control group. Detailed statistics of clean data, sample transcript and FPKM interval from the six microcosms are shown in Dataset 3. Taxonomic annotations are shown in Dataset 4. A total of 3235 differentially expressed genes were identified by RNA-Sequencing analysis (fold change > 2, FDR < 0.05). As shown in the volcano plot (Fig. S2a), only 231 genes were up-regulated, while 3004 genes were down-regulated, which indicated a general inhibitory effect of CIP on microbial transcripts. Unigenes were annotated to functional classification by comparison with the KEGG database. A total of 11,365 orthologs (KOs) were detected (Dataset 5) and consolidated into 344 metabolic pathways at KEGG level 3 (Dataset 6) and 43 metabolic

subsystems at KEGG level 2. These subsystems belong to the six basic metabolic systems of KEGG Level 1. Fig. 5 shows the change in expression abundance of all 23 metabolic subsystems after removal of the subsystems belonging to Human Diseases and Organismal Systems. Four subsystems, Energy metabolism (+19.2% compared to the control, $P < 0.01$), Metabolism of cofactors and vitamins (+53.9%, $P < 0.05$), Metabolism of terpenoids and polyketides (+8.4%, $P < 0.05$), and Membrane Transport (+27.4%, $P < 0.05$), were significantly up-regulated. Seven subsystems, Lipid metabolism (−21.0%, $P < 0.05$), Xenobiotics biodegradation and metabolism (−19.7%, $P < 0.01$), Folding, sorting and degradation (−8.0%, $P < 0.05$), Signal transduction (21.1%, $P < 0.05$), Signaling molecules and interaction (−74.5%, $P < 0.001$), Transport and catabolism (52.7%, $P < 0.001$), and Cellular community (−69.2%, $P < 0.01$), were significantly down-regulated. The remaining 12 subsystems did not change significantly.

3.5. Metabolic pathways in microbial communities in response to CIP treatment

3.5.1. Energy metabolism

In order to analyze the functional changes of the microbial community more specifically, the 11 differentially expressed subsystems were further subdivided into the corresponding KEGG3 metabolic pathways (Fig. 6). Energy metabolism is the most abundant pathway subsystem (20.4% and 24.3% in the control and treatment group) of the microbial community (Fig. 5). Under this subsystem, Oxidative phosphorylation, as the cornerstone of aerobic cell metabolism (Meyer et al., 2009), occupies the most important position (9.1% and 12.0% in the control and treatment group), followed by Photosynthesis (7.3% and 8.2%) and Photosynthesis - antenna proteins (2.1% and 2.6%) (Table S2). Under Photosynthesis - antenna proteins, a serious of genes encoding phycoerythrin (PE), phycocyanin (PC) and allophycocyanin (AP) related protein (*cpe*A, *cpe*C *cpe*D, *cpc*A, *cpc*C, *cpc*E, *cpc*G, *apc*A, *apc*B, *apc*D, *apc*F, etc.) were all up-regulated. The role of these antenna proteins is to absorb and transmit the light energy to the photosynthetic reaction center, allowing photosynthesis to operate smoothly (Collini et al., 2010; Sun et al., 2016). Specifically, light energy is captured by PE and then transmitted to the Photosystem II reaction center complex via PC and AP. These proteins are mainly present in *Cyanobacteria*, *Rhodophyta* and *Cryptophyta* (Yu et al., 2017), and their up-regulation implied that the cyanobacteria tend to produce more light-harvesting pigments for photosynthesis. Photosynthesis is the most important energy conversion and metabolism system for plants (including algae), aiming to generate organic matter and release energy (Nelson and Ben-Shem, 2004; Qian et al., 2016). Under Photosynthesis, a series of genes involved in the modules Photosystem I (M00163) (*psa*C, *psa*D, *psa*L, and *psa*B), Photosystem II (M00161) (*psb*A, *psb*C, *psb*V, *psb*E, and *psb*27), Cytochrome b6f complex (M00162) (*pet*C, *pet*F), and the photosynthetic electron transfer (*pet*E, *pet*H) were up-regulated at different levels. When Photosystem II absorbs light, the excited electrons travel through the cytochrome *b6f* complex to Photosystem I via the photosynthetic electron transport chain (Nelson and Ben-Shem, 2004). Up-regulation of these genes indicated that the photosynthesis of cyanobacteria might be enhanced to some extent. Researchers reported that antibiotics at low concentrations might promote the photosynthesis of cyanobacteria (Liu et al., 2016). It was also found that CIP with concentration as low as 50 ng/L promoted the photosynthesis of *M. aeruginosa* (Liu et al., 2017).

Oxidative phosphorylation is a metabolic pathway in which cells use enzymes to oxidize nutrients, thereby releasing energy for producing adenosine triphosphate (ATP) (Bazil et al., 2016). F-type ATPase is the major producer of ATP, and is present in mitochondria, chloroplasts and bacterial plasma membranes, using proton gradients produced by oxidative phosphorylation (mitochondria) or photosynthesis (chloroplasts). V-type ATPase exists in the vacuoles of plants, fungal cells and some protozoa. The disruption of V-type ATPase function is fatal to almost all eukaryotes (Graham et al., 2003). Under Oxidative phosphorylation, most genes in the module F-type ATPase, prokaryotes and chloroplasts (M00157) were nearly unchanged, while in eukaryotes, most genes in the module F-type ATPase, eukaryotes (M00158) and V-type ATPase, eukaryotes (M00160) were significantly down-regulated (Fig. 7, Dataset 7). The results suggested that ATP production rate in eukaryotes might be inhibited, while prokaryotes appeared to be less affected. Two pathways associated with the microbial biogeochemical cycles, Sulfur metabolism (−50.1%, $P < 0.05$) and Nitrogen metabolism (−25.6%, $P < 0.05$) were significantly down-regulated (Table S2). Córdovakreylos and Scow (2007) found a selective effect of CIP on

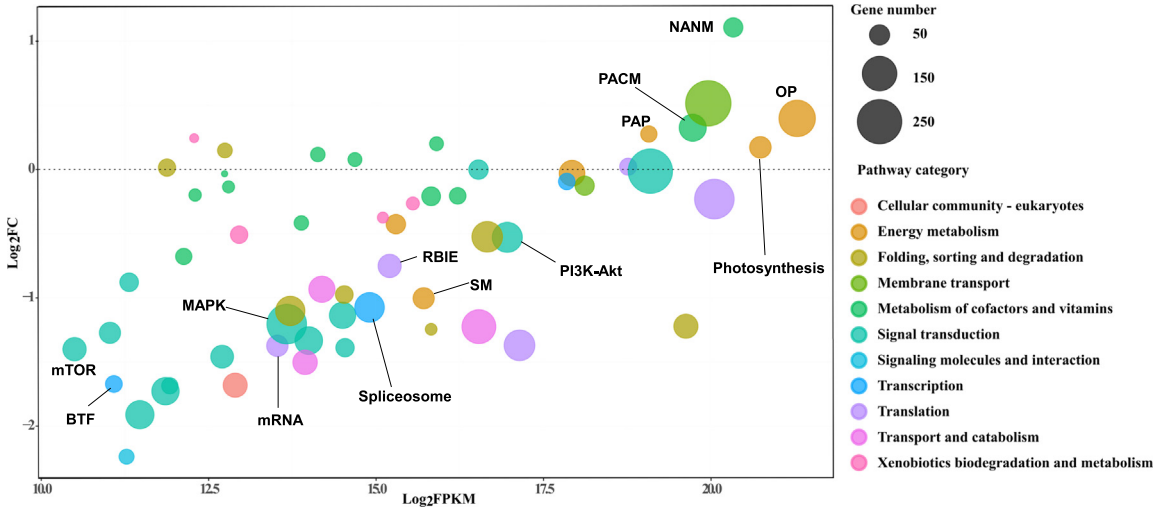

Fig. 6. Color-coded scatter plot of metabolic pathways at KEGG 3 level. Pathways are grouped into different categories based on KEGG classification. Log_2FC is the fold change in transcript abundance between the control group and the treatment group in log scale. Log_2FPKM is the transcript FPKM value of the treatment group in log scale. Circle size represents the gene number in the metabolic pathway. Selected pathways are annotated as follows: NANM, Nicotinate and nicotinamide metabolism (ko00190); OP, Oxidative phosphorylation (ko00196); PACM, Porphyrin and chlorophyll metabolism (ko00680); Photosynthesis (ko00760); PAP, Photosynthesis - antenna proteins (ko00196); PI3K-Akt, PI3K-Akt signaling pathway (ko04024); RBIE, Ribosome biogenesis in eukaryotes (ko04152); SM, Sulfur metabolism (ko04071); Spliceosome (ko04668); MAPK, MAPK signaling pathway (ko04140); mRNA, mRNA surveillance pathway (ko04130); mTOR, mTOR signaling pathway (ko04122); BTF, Basal transcription factors (ko00983).

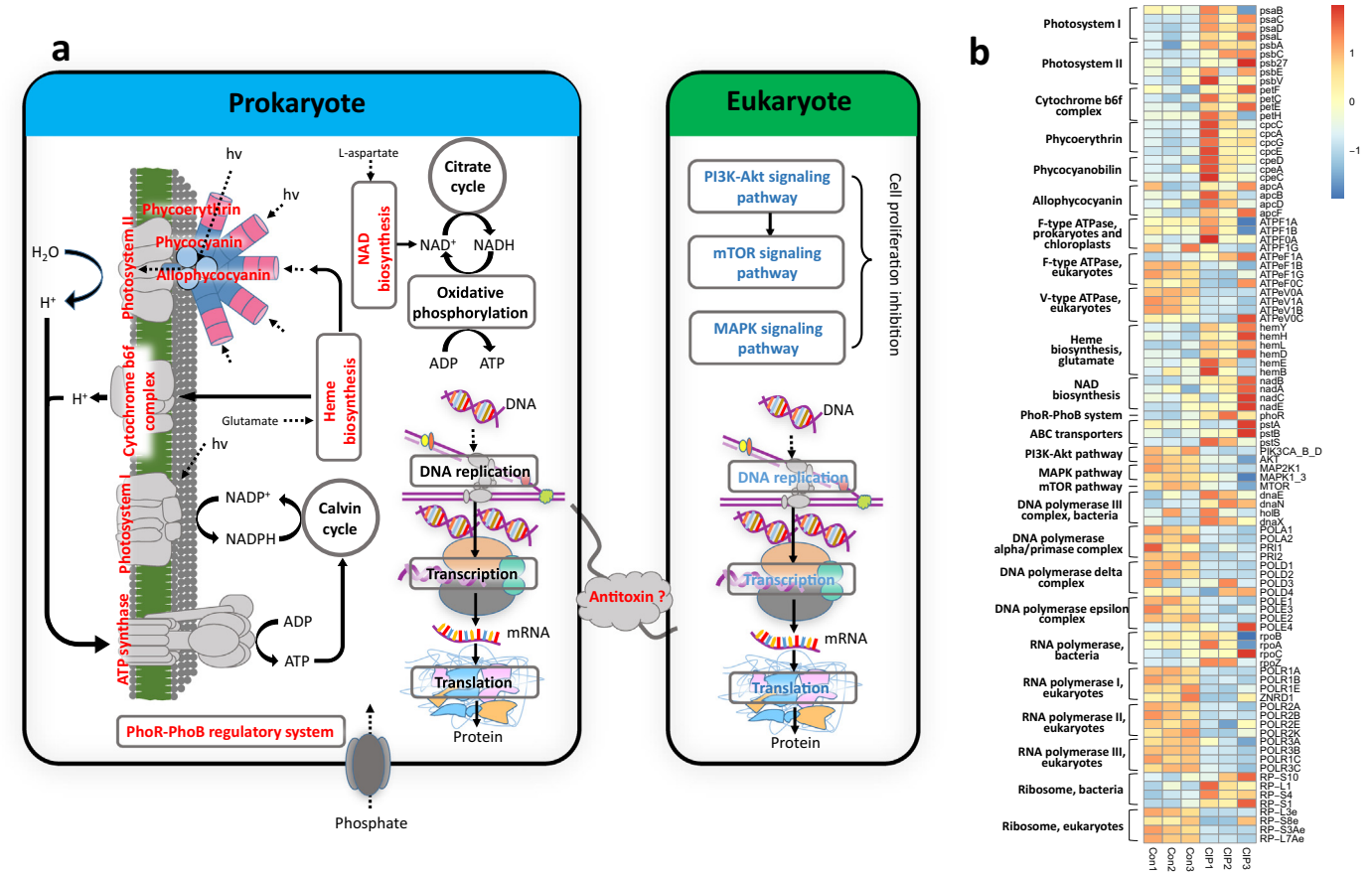

Fig. 7. The overall changes in the metabolic pathways after CIP treatment. (a) Different changes in prokaryotes and eukaryotes. The character in red represents up-regulation of the pathway in the treatment group compared to the control group, and character in black or blue represents no significant change or down-regulation of the pathway. (b) Heatmap of transcript proportions in the control and treatment samples in KEGG level 4. Relative expression values are scaled by *Z*-score per transcript. (For interpretation of the references to color in this figure legend, the reader is referred to the web version of this article.)

sulfate reducers and Gram-negative bacteria, which converted the microbial community from an acetate-utilizing system (dominated by *Desulfobacter*) to a system that is capable of utilizing more complex carbon substrates. This is consistent with the suppression of the Sulfur metabolism pathway in our study. Under this pathway, a gene *sir* (K00392), which encodes sulfite reductase (ferredoxin) (EC:1.8.7.1), was significantly down-regulated (−46.5%, $P < 0.05$) (Fig. 7, Dataset 7), indicating that the sulfate assimilation of cyanobacteria might be inhibited.

3.5.2. Metabolism of cofactors and vitamins

Under the Metabolism of cofactors and vitamins subsystem, Porphyrin and chlorophyll metabolism (+25.3%, $P < 0.05$) and Nicotinate and nicotinamide metabolism (+115.5%, $P < 0.05$) were significantly up-regulated (Table S2). Heme is the precursor for cytochromes, chlorophylls, phycobilins, and vitamin B_{12} (Oborník and Green, 2005). Under Porphyrin and chlorophyll metabolism, genes (PPOX, *hem*H, *hem*L *cob*A-*hem*D, *hem*E, *hem*B, *hem*D) in the module Heme biosynthesis, glutamate (M00121), encoding enzymes catalyzing the heme biosynthesis from L-Glutamate, were all up-regulated. Enhancement of heme biosynthesis could be beneficial to the synthesis of cyanobacterial photosynthetic pigments, and further be beneficial to the photosynthesis (Gong et al., 2017). Under Nicotinate and nicotinamide metabolism, four genes (*nad*B, *nad*A, *nad*C, *nad*E) in the module NAD biosynthesis (M00115), encoding enzymes catalyzing the de novo biosynthesis of nicotinamide adenine dinucleotide (NAD) from L-aspartate, were up-regulated (Fig. 7, Dataset 7). NAD is an important cofactor that is present in all living organisms and plays an important role in many cellular processes, including protection against cell injuries (Liang et al., 2017a) and environmental stress (Hashida et al., 2009). The up-regulation of NAD biosynthesis might be the self-defense of cyanobacteria against CIP stress.

3.5.3. Signal transduction

Signal transduction is the process by which a chemical or physical signal is transmitted through a cell as a series of molecular events. These molecular events are the basic mechanisms controlling cell growth, proliferation, metabolism and many other processes. Two-component signal transduction systems enable bacteria to sense, respond, and adapt to changes in their environment or in their intracellular state. Under the Two-component system, a main gene *pho*R (+74.0%, $P < 0.05$) in the module PhoR-PhoB (phosphate starvation response) two-componsent regulatory system (M00434) was significantly up-regulated. In addition, under pathway ABC transporters, genes (*pst*A, *pst*B, *pst*S) under the bacterial module Phosphate transport system (M00222) were also up-regulated (Fig. 7, Dataset 7). This is a signal that the bacteria were experiencing phosphate starvation, and enhanced their phosphate transport system. Apart from the Two-component system, the genes were mostly down-regulated in other pathways under the Signal transduction subsystem. These pathways are usually described in eukaryotes. The PI3K-Akt signaling pathway (−30.7%, $P < 0.05$) was significantly down-regulated. Under this pathway, gene AKT (−53.7%, $P < 0.05$), encoding RAC serine/threonine-protein kinase (EC:2.7.11.1), was significantly down-regulated. The PI3K/AKT/mTOR pathway is an important intracellular signaling pathway in the regulation of the cell cycle. PI3K activation phosphorylates and activates AKT, which has many downstream effects such as activation of mTOR (Schultze et al., 2012). It was found that the

mTOR signaling pathway (−62.1%, P < 0.05) was significantly down-regulated. Furthermore, the MAPK signaling pathway (−56.6%, P < 0.05) was also significantly down-regulated (Table S2, Fig. 7, Dataset 7). This pathway is associated with cell proliferation, differentiation, migration, senescence and apoptosis (Sun et al., 2015). Inhibition of the MAPK signaling pathway can inhibit cell growth and induce apoptosis (Cha et al., 2012). Although these pathways are usually described in large mammals such as humans and rats, they also exist in multicellular aquatic organisms such as rotifers (Lee et al., 2017). These results suggested that the cell proliferation in multicellular eukaryotes was likely inhibited after CIP exposure.

3.5.4. DNA replication, transcription and translation

Under Replication and repair, the DNA replication pathway was significantly down-regulated (−21.8%, P < 0.05). Under this pathway, genes (*dna*N, *dna*E, *dna*X, *dna*Q, *hol*A, *hol*B, *hol*C) in module DNA polymerase III complex, bacteria (M00260) were all slightly up-regulated. DNA polymerase III is the major enzyme complex involved in prokaryotic DNA leader strand replication (Kelman and O'Donnell, 1995). However, genes in the eukaryotic modules DNA polymerase alpha/primase complex (M00261), DNA polymerase delta complex (M00262), and DNA polymerase epsilon complex (M00263) were almost all significantly down-regulated. DNA polymerase synthesizes DNA molecules from deoxyribonucleotides. This enzyme is essential for DNA replication. While in eukaryotes, three DNA polymerases (alpha, delta, and epsilon) with the same function have been identified (Izumi et al., 2011). Besides, under the RNA polymerase pathway, genes in the eukaryote-related modules RNA polymerase I, eukaryotes (M00182), RNA polymerase II, eukaryotes (M00181), and RNA polymerase III, eukaryotes (M00183) were almost all significantly down-regulated, while genes (*rpo*B, *rpo*A, *rpo*C, *rpo*Z, etc.) in the prokaryotic module RNA polymerase, bacteria (M00183) were unchanged. RNA polymerase is required for the transcriptional initiation of bacteria and eukaryotes (Saecker et al., 2011). In bacteria, the same RNA polymerase catalyzes the synthesis of messenger RNA (mRNA) and non-coding RNA. In eukaryotes there are many types of RNA polymerases that are responsible for the synthesis of different RNA subgroups (Herr et al., 2005). Besides, basic transcription factors, which bind to specific sites on the DNA (promoter) and activate transcription of genetic information from DNA to mRNA, are also essential for the transcriptional initiation. The Basal transcription factors pathway (−68.6%, P < 0.001) was down-regulated as well. In addition, it was found that spliceosome was also significantly down-regulated (−52.5%, P < 0.01). Spliceosome is a large and complex molecular machine found primarily within the nucleus of eukaryotic cells (Plaschka et al., 2017). Under Translation, RNA transport (−61.3%, P < 0.001), mRNA surveillance pathway (−61.4%, P < 0.001), and Ribosome biogenesis in eukaryotes (−40.6%, P < 0.05) were all significantly down-regulated, while Ribosome (−14.8, P > 0.05) was only slightly and non-significantly down-regulated. RNA transport process delivers a different category of RNA from the nucleus to the cytoplasm, which is the basis of gene expression (Köhler and Hurt, 2007). The mRNA surveillance pathway is an intracellular monitoring mechanism for detecting and degrading abnormal mRNA (Nadia et al., 2006). Ribosomes are the workplaces of protein biosynthesis, the process of translating mRNA into proteins (Lafontaine and Tollervey, 2001). These three important pathways affect the productivity and quality of the RNA translation process. Similarly, under Ribosome, genes in the module Ribosome, eukaryotes (M00177) were mostly down-regulated, while genes in the module Ribosome, bacteria (M00178) were mostly unchanged (Fig. 7, Dataset 7). Disorders in these important RNA translation processes suggested impaired protein biosynthesis ability in eukaryotes. To sum up, these results indicated that a series of life processes from DNA replication to RNA translation in eukaryotes were all seriously affected, while prokaryotes showed no significant changes in these processes.

3.6. Environmental implications

Microorganisms, including algae, are sensitive to contaminants and are indicators of the condition of ecosystems (Lu et al., 2018c; Zhang et al., 2018). The metatranscriptomic analyses bring new insights into the impacts of CIP (7 μg/L) in freshwater microbial communities. Although CIP did not cause severe toxic effects on microbial communities, exposure to CIP resulted in down-regulation of various genes and pathways in the treatment group, with a few up-regulated pathways observed (Fig. 6, Table S2). These up-regulated pathways might be the key of microbial tolerance to the indirect effects of CIP exposure. Bacteria, mainly cyanobacteria, generated a series of stress responses in metabolism and gene expression, e.g., the strengthening of the two-component regulatory system and the photosystem, which might be a way for bacteria to withstand CIP. The above phenomena indicate that the bacteria in microcosm were sufficiently adaptive to cope with stress induced by trace amounts of CIP. However, in eukaryotes, the replication, transcription, translation and cell proliferation were all suppressed. CIP is known as a bacterial DNA gyrase inhibitor and has been shown to be rather non-toxic to eukaryotic organisms (Ebert et al., 2011; Wallace et al., 2018).

In the aquatic environment, plankton commonly relies on metabolites excreted by other species (Harcombe et al., 2018). Adamowicz et al. (2018) clearly showed that cross-feeding can alter the tolerance to antibiotics in a variety of systems. Alternatively, the community tolerance to a certain antibiotic tends to be higher than that of a sensitive species in a monoculture, which is also called the “community protection” hypothesis. Although 7 μg/L of CIP was not mortal to cyanobacteria, it still could inhibit most of them to a certain degree (Fig. S1b). But interestingly, the present study showed that trace amounts of CIP in a freshwater microcosm were tolerable for cyanobacteria and unexpectedly inhibited eukaryotic growth, which is the exact opposite of the anti-bacterial classification of CIP. Due to the complexity of microbial communities (there exist not only cyanobacteria, but also heterotrophic bacteria, eukaryotic algae, fungi, zooplankton and other species), the enhanced tolerance of cyanobacteria to CIP was likely to be associated with microbial mutualisms.

Besides mutualisms, antagonistic interactions in microbial communities are also ubiquitous, and there is evidence that bacteria can affect eukaryotes by secreting certain secondary metabolites (Song et al., 2017). We found that two major genes (*parD1_3_4* and *yefM*) encoding antitoxins were up-regulated by 423% and 47% (Fig. 7, Dataset 7). Because antitoxins are ubiquitous in bacteria and archaea, they can neutralize certain toxins and act as a metabolic regulator of growth in stress physiology (Hayes and Van, 2011). However, many antitoxins can repress transcription and are toxic to other microorganisms (Kamphuis et al., 2007). The bacteria might enhance the production of various compounds like antitoxin in response to CIP stress, which might in turn impact the growth of eukaryotes as well. Similar mechanisms of action between microorganisms might be the reason of the observed anomalies in the present study.

In any case, the effects of trace amounts of CIP on the eukaryotic and prokaryotic community diversity as well as the changes in community function may affect the stability of aquatic ecosystems.

4. Conclusions

The current study demonstrated that 7 μg/L of CIP had unexpected effects on the taxonomy and function of a plankton community. The eukaryotic community was affected more than the bacterial community. Meta-transcriptomic results showed that gene expressions related to replication, transcription, translation and cell proliferation in eukaryotes were all suppressed, while the bacteria were not significantly affected in any of these aspects (Fig. 7). Cyanobacteria might strengthen their two-component regulatory system and the photosystem to cope with CIP. We hypothesize that reciprocal and antagonistic interactions

in the microcosm both contribute to this interesting phenomenon: i) Benefiting from cross-feeding with other species, cyanobacteria enhanced their tolerance to CIP, ii) The bacteria might excrete certain compounds to withstand CIP stress, but the secreted substances happened to affect eukaryotes. This study thus indicates that the aquatic ecotoxicity of trace concentrations of CIP is much more complicated in a microcosm than in monocultures. The uncertain consequence of all kinds of antibiotic contamination in plankton communities indicates that even traces of antibiotic residues could also pose unknown risks. Future studies will focus on the details of reciprocal and antagonistic interaction model within the plankton community under CIP stress. The effects of multiple antibiotics on aquatic environments also need extensive attention, as well as their combined toxicity with other pollutants.

Conflict of interest

The authors declare no conflict of interests.

Acknowledgments

This work was financially supported by National Key Research and Development Program of China (2017YFD0200503), National Natural Science Foundation of China (21577128, 21777144), and Chinese Postdoctoral Science Foundation (2018M632502).

Appendix A. Supplementary data

Supplementary data to this article can be found online at https://doi.org/10.1016/j.envint.2019.02.050.

References

Adamowicz, E.M., Flynn, J., Hunter, R.C., Harcombe, W.R., 2018. Cross-feeding modulates antibiotic tolerance in bacterial communities. ISME J. 12, 2723–2735.
An, X.L., Chen, Q.L., Zhu, D., Zhu, Y.G., Gillings, M.R., Su, J.Q., 2018a. Impact of wastewater treatment on the prevalence of integrons and the genetic diversity of integron gene cassettes. Appl. Environ. Microbiol. 84, e02766-17.
An, X.L., Su, J.Q., Li, B., Ouyang, W.Y., Zhao, Y., Chen, Q.L., Cui, L., Chen, H., Gillings, M.R., Zhang, T., 2018b. Tracking antibiotic resistome during wastewater treatment using high throughput quantitative PCR. Environ. Int. 117, 146–153.
Barboza, G.F.O., Gorlach-Lira, K., Sassi, C.F.C., Sassi, R., 2017. Microcystins production and antibacterial activity of cyanobacterial strains of *Synechocystis*, *Synechococcus* and *Romeria* from water and coral reef organisms (Brazil). Rev. Biol. Trop. 65, 890–899.
Bazil, J.N., Beard, D.A., Vinnakota, K.C., 2016. Catalytic coupling of oxidative phosphorylation, ATP demand, and reactive oxygen species generation. Biophys. J. 110, 962–971.
Ben, W., Zhu, B., Yuan, X., Zhang, Y., Yang, M., Qiang, Z., 2018. Occurrence, removal and risk of organic micropollutants in wastewater treatment plants across China: comparison of wastewater treatment processes. Water Res. 130, 38–46.
Cha, J.H., Choi, Y.J., Cha, S.H., Choi, C.H., Cho, W.H., 2012. Allicin inhibits cell growth and induces apoptosis in U87MG human glioblastoma cells through an ERK-dependent pathway. Oncol. Rep. 28, 41–48.
Collini, E., Wong, C.Y., Wilk, K.E., Curmi, P.M.G., Brumer, P., Scholes, G.D., 2010. Coherently wired light-harvesting in photosynthetic marine algae at ambient temperature. Nature 463, 644–647.
Córdovakreylos, A.L., Scow, K.M., 2007. Effects of ciprofloxacin on salt marsh sediment microbial communities. ISME J. 1, 585–595.
Dirren, S., Pitsch, G., Silva, M.O.D., Posch, T., 2017. Grazing of *Nuclearia thermophila* and *Nuclearia delicatula* (*Nucleariidae*, *Opisthokonta*) on the toxic cyanobacterium *Planktothrix rubescens*. Eur. J. Protistol. 60, 87–101.
Doronina, N.V., Darmaeva, T.D., Trotsenko, Y.A., 2003. *Methylophaga alcalica* sp. nov., a novel alkaliphilic and moderately halophilic, obligately methylotrophic bacterium from an East Mongolian saline soda lake. Int. J. Syst. Evol. Micr. 53, 223–229.
Du, B., Zhang, Z., Liu, W., Ye, Y., Lu, T., Zhou, Z., Li, Y., Fu, Z., Qian, H., 2019. Acute toxicity of the fungicide azoxystrobin on the diatom *Phaeodactylum tricornutum*. Ecotoxicol. Environ. Saf. 168, 72–79.
Ebert, I., Bachmann, J., Kühnen, U., Küster, A., Kussatz, C., Maletzki, D., Schlüter, C., 2011. Toxicity of the fluoroquinolone antibiotics enrofloxacin and ciprofloxacin to photoautotrophic aquatic organisms. Environ. Toxicol. Chem. 30, 2786–2792.
Gong, W., Browne, J., Hall, N., Schruth, D., Paerl, H., Marchetti, A., 2017. Molecular insights into a dinoflagellate bloom. ISME J. 11, 439–452.
Graham, L.A., Flannery, A.R., Stevens, T.H., 2003. Structure and assembly of the yeast V-ATPase. J. Bioenerg. Biomembr. 35, 301–312.
Hallingsørensen, B., Lützhøft, H.C.H., Andersen, H.R., Ingerslev, F., 2000. Environmental risk assessment of antibiotics: comparison of mecillinam, trimethoprim and ciprofloxacin. J. Antimicrob. Chemother. 46, 53–58.
Hanna, N., Sun, P., Sun, Q., Li, X., Yang, X., Ji, X., Zou, H., Ottoson, J., Nilsson, L.E., Berglund, B., 2018. Presence of antibiotic residues in various environmental compartments of Shandong province in eastern China: its potential for resistance development and ecological and human risk. Environ. Int. 114, 131–142.
Harcombe, W.R., Chacón, J.M., Adamowicz, E.M., Chubiz, L.M., Marx, C.J., 2018. Evolution of bidirectional costly mutualism from byproduct consumption. P. Natl. Acad. Sci. USA. 115, 12000–12004.
Hashida, S.N., Takahashi, Hideyuki, Uchimiya, H., 2009. The role of NAD biosynthesis in plant development and stress responses. Ann. Bot. 103, 819–824.
Hayes, F., Van, M.L., 2011. Toxins-antitoxins: diversity, evolution and function. Crit. Rev. Biochem. Mol. Biol. 46, 386–408.
Herr, A.J., Jensen, M.B., Dalmay, T., Baulcombe, D.C., 2005. RNA polymerase IV directs silencing of endogenous DNA. Science 308, 118–120.
Izumi, M., Kunkel, T.A., Carr, A.M., 2011. The major roles of DNA polymerases epsilon and delta at the eukaryotic replication fork are evolutionarily conserved. PLoS Genet. 7, e1002407.
Jia, Y., Khanal, S.K., Shu, H., Zhang, H., Chen, G.H., Lu, H., 2018. Ciprofloxacin degradation in anaerobic sulfate-reducing bacteria (SRB) sludge system: mechanism and pathways. Water Res. 136, 64–74.
Jiang, Y., Li, M., Guo, C., An, D., Xu, J., Zhang, Y., Xi, B., 2014. Distribution and ecological risk of antibiotics in a typical effluent-receiving river (Wangyang River) in north China. Chemosphere 112, 267–274.
Johansson, C.H., Janmar, L., Backhaus, T., 2014. Toxicity of ciprofloxacin and sulfamethoxazole to marine periphytic algae and bacteria. Aquat. Toxicol. 156, 248–258.
Kamphuis, M.B., Monti, M.C., Rh, V.D.H., Santos-Sierra, S., Folkers, G.E., Lemonnier, M., Díaz-Orejas, R., Heck, A.J., Boelens, R., 2007. Interactions between the toxin kid of the bacterial *par*D system and the antitoxins Kis and MazE. Proteins 67, 219–231.
Kasprzak, P., Padisák, J., Koschel, R., Krienitz, L., Gervais, F., 2008. Chlorophyll *a* concentration across a trophic gradient of lakes: An estimator of phytoplankton biomass? Limnologica 38, 327–338.
Keeney, K.M., Yuristdoutsch, S., Arrieta, M.C., Finlay, B.B., 2014. Effects of antibiotics on human microbiota and subsequent disease. Annu. Rev. Microbiol. 68, 217–235.
Kelman, Z., O'Donnell, M., 1995. DNA polymerase III holoenzyme: structure and function of a chromosomal replicating machine. Annu. Rev. Biochem. 64, 171–200.
Köhler, A., Hurt, E., 2007. Exporting RNA from the nucleus to the cytoplasm. Nat. Rev. Mol. Cell Bio. 8, 761–773.
Kulesza, S.B., Maguire, R.O., Xia, K., Cushman, J., Knowlton, K., Ray, P., 2016. Manure injection affects the fate of pirlimycin in surface runoff and soil. J. Environ. Qual. 45, 511–518.
Lafontaine, D.L.J., Tollervey, D., 2001. The function and synthesis of ribosomes. Nat. Rev. Mol. Cell Bio. 2, 514–520.
Lee, Y.H., Kim, D.H., Kang, H.M., Wang, M., Jeong, C.B., Lee, J.S., 2017. Adverse effects of methylmercury (MeHg) on life parameters, antioxidant systems, and MAPK signaling pathways in the rotifer *Brachionus koreanus* and the copepod *Paracyclopina nana*. Aquat. Toxicol. 190, 181–189.
Letcher, P.M., Longcore, J.E., Quandt, C.A., Leite, D.D.S., James, T.Y., Powell, M.J., 2017. Morphological, molecular, and ultrastructural characterization of *Rozella rhizoclosmatii*, a new species in *Cryptomycota*. Fungal Biol. 121, 1–10.
Liang, M., Yin, X.L., Wang, L.Y., Yin, W.H., Song, N.Y., Shi, H.B., Li, C.Y., Yin, S.K., 2017a. NAD^+ attenuates bilirubin-induced hyperexcitation in the ventral cochlear nucleus by inhibiting excitatory neurotransmission and neuronal excitability. Front. Cell. Neurosci. 11, 21.
Liang, Y., Ouyang, K., Chen, X., Su, Y., Yang, J., 2017b. Life strategy and grazing intensity responses of *Brachionus calyciflorus* fed on different concentrations of microcystin-producing and microcystin-free *Microcystis aeruginosa*. Sci. Rep. 7, 43127.
Liao, K., Bai, Y., Huo, Y., Jian, Z., Hu, W., Zhao, C., Qu, J., 2018. Integrating microbial biomass, composition and function to discern the level of anthropogenic activity in a river ecosystem. Environ. Int. 116, 147–155.
Liu, Y., Chen, S., Zhang, J., Gao, B., 2016. Growth, microcystin-production and proteomic responses of *Microcystis aeruginosa* under long-term exposure to amoxicillin. Water Res. 93, 141–152.
Liu, Y., Chen, S., Zhang, J., Li, X., Gao, B., 2017. Stimulation effects of ciprofloxacin and sulphamethoxazole in *Microcystis aeruginosa* and isobaric tag for relative and absolute quantitation-based screening of antibiotic targets. Mol. Ecol. 26, 689–701.
Lu, T., Zhu, Y., Xu, J., Ke, M., Zhang, M., Tan, C., Fu, Z., Qian, H., 2018a. Evaluation of the toxic response induced by azoxystrobin in the non-target green alga *Chlorella pyrenoidosa*. Environ. Pollut. 234, 379–388.
Lu, T., Ke, M.J., Peijnenburg, W.J.G.M., Zhu, Y.C., Zhang, M., Sun, L.W., Fu, Z.W., Qian, H.F., 2018b. Investigation of rhizospheric microbial communities in wheat, barley, and two rice varieties at the seedling stage. J. Agr. Food Chem. 66, 2645–2653.
Lu, T., Ke, M.J., Lavoie, M., Jin, Y., Fan, X., Zhang, Z., Fu, Z., Sun, L., Gillings, M., Peñuelas, J., Qian, H., Zhu, Y.G., 2018c. Rhizosphere microorganisms can influence the timing of plant flowering. Microbiome. 6, 231.
Meyer, E.H., Tomaz, T., Carroll, A.J., Estavillo, G., Delannoy, E., Tanz, S.K., Small, I.D., Pogson, B.J., Millar, A.H., 2009. Remodeled respiration in *ndufs4* with low phosphorylation efficiency suppresses *Arabidopsis* germination and growth and alters control of metabolism at night. Plant Physiol. 151, 603–619.
Mou, X., Lu, X., Jacob, J., Sun, S., Heath, R., 2013. Metagenomic identification of bacterioplankton taxa and pathways involved in microcystin degradation in lake erie. PLoS One 8, e61890.
Nadia, A., Sachs, M.S., Allan, J., 2006. Early nonsense: mRNA decay solves a translational problem. Nat. Rev Mol. Cell Biol. 7, 415–425.
Nelson, N., Ben-Shem, A., 2004. The complex architecture of oxygenic photosynthesis.

Nat. Rev. Mol. Cell Bio. 5, 971–982.
Oborník, M., Green, B.R., 2005. Mosaic origin of the heme biosynthesis pathway in photosynthetic eukaryotes. Mol. Biol. Evol. 22, 2343–2353.
Oudra, B., Loudiki, M., Vasconcelos, V., Sabour, B., Sbiyyaa, B., Oufdou, K., Mezrioui, N., 2002. Detection and quantification of microcystins from cyanobacteria strains isolated from reservoirs and ponds in Morocco. Environ. Toxicol. 17, 32–39.
Plaschka, C., Lin, P.C., Nagai, K., 2017. Structure of a pre-catalytic spliceosome. Nature 546, 617–621.
Qian, H., Zhu, K., Lu, H., Lavoie, M., Chen, S., Zhou, Z., Deng, Z., Chen, J., Fu, Z., 2016. Contrasting silver nanoparticle toxicity and detoxification strategies in *Microcystis aeruginosa* and *Chlorella vulgaris*: new insights from proteomic and physiological analyses. Sci. Total Environ. 572, 1213–1221.
Qian, H., Lu, T., Song, H., Lavoie, M., Xu, J., Fan, X., Pan, X., 2017. Spatial variability of cyanobacteria and heterotrophic bacteria in Lake Taihu (China). Bull. Environ. Contam. Toxicol. 99, 1–5.
Qian, H., Zhu, Y., Chen, S., Jin, Y., Lavoie, M., Ke, M., Fu, Z., 2018. Interacting effect of diclofop-methyl on the rice rhizosphere microbiome and denitrification. Pestic. Biochem. Physiol. 146, 90–96.
Saecker, R.M., Record Jr., M.T., Dehaseth, P.L., 2011. Mechanism of bacterial transcription initiation: RNA polymerase-promoter binding, isomerization to initiation-competent open complexes, and initiation of RNA synthesis. J. Mol. Biol. 412, 754–771.
Schultze, S.M., Hemmings, B.A., Niessen, M., Tschopp, O., 2012. PI3K/AKT, MAPK and AMPK signalling: protein kinases in glucose homeostasis. Expert Rev. Mol. Med. 14, 1.
Silveira, S.T., Burkert, J.F.M., Costa, J.A.V., Burkert, C.A.V., Kalil, S.J., 2007. Optimization of phycocyanin extraction from *Spirulina platensis* using factorial design. Bioresour. Technol. 98, 1629–1634.
Song, H., Lavoie, M., Fan, X., Tan, H., Liu, G., Xu, P., Fu, Z., Paerl, H.W., Qian, H., 2017. Allelopathic interactions of linoleic acid and nitric oxide increase the competitive ability of *Microcystis aeruginosa*. ISME J. 11, 1865–1876.
Su, H., Hu, X., Xu, Y., Xu, W., Huang, X., Wen, G., Yang, K., Li, Z., Cao, Y., 2018. Persistence and spatial variation of antibiotic resistance genes and bacterial populations change in reared shrimp in South China. Environ. Int. 119, 327–333.
Sun, Y., Liu, W.Z., Liu, T., Feng, X., Yang, N., Zhou, H.F., 2015. Signaling pathway of MAPK/ERK in cell proliferation, differentiation, migration, senescence and apoptosis. J. Recept. Sig. Transd. 35, 600–604.
Sun, C., Chen, S., Jin, Y., Song, H., Ruan, S., Fu, Z., et al., 2016. Effects of the herbicide imazethapyr on photosynthesis in PGR5- and NDH-deficient *Arabidopsis thaliana* at the biochemical, transcriptomic, and proteomic levels. J. Agric. Food Chem. 64, 4497–4504.
Szabó, K.É., Itor, P., 2007. Importance of rare and abundant populations for the structure and functional potential of freshwater bacterial communities. Aquat. Microb. Ecol. 183, 5223–5229.
Tahrani, L., Van, L.J., Ben, M.H., Reyns, T., 2016. Occurrence of antibiotics in pharmaceutical industrial wastewater, wastewater treatment plant and sea waters in Tunisia. J. Water Health 14, 208–213.
Visser, P.M., Verspagen, J.M.H., Sandrini, G., Stal, L.J., Matthijs, H.C.P., Davis, T.W., Paerl, H.W., Huisman, J., 2016. How rising CO_2 and global warming may stimulate harmful cyanobacterial blooms. Harmful Algae 54, 145–159.
Wallace, M.D., Waraich, N.F., Debowski, A.W., Corral, M.G., Maxwell, A., Mylne, J.S., Stubbs, K.A., 2018. Developing ciprofloxacin analogues against plant DNA gyrase: a novel herbicide mode of action. Chem. Commun. 54, 1869–1872.
Wang, Y., Eustance, E., Castillo-Keller, M., Sommerfeld, M., 2017. Evaluation of chemical treatments for control of ciliate grazers in algae cultures: a site study. J. Appl. Phycol. 29, 2761–2770.
Wei, R., Ge, F., Chen, M., Wang, R., 2012. Occurrence of ciprofloxacin, enrofloxacin, and florfenicol in animal wastewater and water resources. J. Environ. Qual. 41, 1481–1486.
Wilson, B.A., Smith Jr., V.H., deNoyelles, F., Larive, C.K., 2003. Effects of three pharmaceutical and personal care products on natural freshwater algal assemblages. Environ. Sci. Technol. 37, 1713–1719.
Woźniak, M., Bradtke, K., Darecki, M., Krężel, A., 2016. Empirical model for phycocyanin concentration estimation as an indicator of cyanobacterial bloom in the optically complex coastal waters of the Baltic Sea. Remote Sens. 8, 212.
Xu, H., Paerl, H.W., Qin, B., Zhu, G., Gaoa, G., 2010. Nitrogen and phosphorus inputs control phytoplankton growth in eutrophic Lake Taihu, China. Limnol. Oceanogr. 55, 420–432.
Yu, P., Wu, Y., Wang, G., Jia, T., Zhang, Y., 2017. Purification and bioactivities of phycocyanin. Crit. Rev. Food Sci. Nutr. 57, 3840–3849.
Zhang, Q.Q., Ying, G.G., Pan, C.G., Liu, Y.S., Zhao, J.L., 2015. Comprehensive evaluation of antibiotics emission and fate in the river basins of China: source analysis, multimedia modeling, and linkage to bacterial resistance. Environ. Sci. Technol. 49, 6772–6782.
Zhang, R., Zhang, R., Zou, S., Yang, Y., Li, J., Wang, Y., Yu, K., Zhang, G., 2017. Occurrence, distribution and ecological risks of fluoroquinolone antibiotics in the Dongjiang river and the Beijiang river, pearl river delta, South China. Bull. Environ. Contam. Toxicol. 99, 46–53.
Zhang, Q., Qu, Q., Lu, T., Ke, M., Zhu, Y., Zhang, M., Zhang, Z., Du, B., Pan, X., Sun, L., Qian, H., 2018. The combined toxicity effect of nanoplastics and glyphosate on *Microcystis aeruginosa* growth. Environ. Pollut. 243, 1106–1112.
Zheng, Q., Zhang, R., Wang, Y., Pan, X., Tang, J., Zhang, G., 2012. Occurrence and distribution of antibiotics in the Beibu Gulf, China: impacts of river discharge and aquaculture activities. Mar. Environ. Res. 78, 26–33.
Zhu, Y.G., Johnson, T.A., Su, J.Q., Qiao, M., Guo, G.X., Stedtfeld, R.D., Hashsham, S.A., Tiedje, J.M., 2013. Diverse and abundant antibiotic resistance genes in Chinese swine farms. P. Natl. Acad. Sci. USA. 110, 3435–3440.
Zhu, Y.G., Gillings, M., Simonet, P., Stekel, D., Banwart, S., Penuelas, J., 2017. Microbial mass movements. Science 357, 1099–1100.